



Asphalt mixture design for porous ultra-thin overlay

Ziming Liu^a, Xinming Wang^b, Sang Luo^{c,*}, Xu Yang^d, Qiang Li^e

^a School of Transportation, Southeast University, Nanjing 210096, China

^b Suzhou Channel Management, Suzhou 215000, China

^c Intelligent Transportation Research Center, Southeast University, Nanjing 210096, China

^d Department of Civil Engineering, Monash University, Victoria 3800, Australia

^e School of Civil Engineering, Nanjing Forestry University, Nanjing 210037, China



HIGHLIGHTS

- A porous ultra-thin overlay (PUTO) was proposed.
- High-viscosity asphalt was prepared.
- The gradation of PUTO is designed.
- The performance of PUTO is verified.

ARTICLE INFO

Article history:

Received 30 March 2019

Received in revised form 6 May 2019

Accepted 7 May 2019

Available online 16 May 2019

Keywords:

Design asphalt mixture

Porous ultra-thin overlay

High-viscosity asphalt

Design gradation

Performance verification

ABSTRACT

In order to design a porous ultra-thin overlay (PUTO) asphalt mixture, two high-viscosity modifiers and two blended asphalts were used to prepare high-viscosity asphalt. Dynamic shear rheology (DSR) tests, 60 °C dynamic viscosity tests, Fourier transform infrared spectroscopy (FTIR) tests and physical properties tests were used to study the modification effect and modification mechanism of high-viscosity asphalt. Next, based on existing gradation design methods, two types of gradation, coarse and fine, were designed for PUTO. In addition, based on the results of draindown and Cantabro tests, the optimal asphalt-aggregate ratio was determined. Finally, the performance of the designed PUTO asphalt mixture was verified. The results show that with the increase of the amount of high-viscosity modifier, the complex shear modulus and anti-rutting factors of the four kinds of high-viscosity asphalt gradually increase, while their phase angles gradually decrease. Only SBS-I (with high-viscosity modifier contents of 14% and 16%) and SBS-II (with high-viscosity modifier contents of 14% and 16%) high-viscosity asphalt have a 60 °C dynamic viscosity exceeding 100,000 Pa·s. The main component of the high-viscosity modifier for the modification of the original asphalt is thermoplastic rubber, which forms a polymer network structure between the polymer in the high-viscosity modifier and the asphalt component, which is reflected in the infrared spectrum. That is, there is a significant characteristic absorption peak at 966 cm⁻¹ in the fingerprint vibration spectrum region (1500–600 cm⁻¹). After the high-viscosity modifier content reaches 14%, the penetration of SBS-I and SBS-II high-viscosity asphalt decreases, and their growth trends of ductility and softening point also slow. Considering the total cost, when the SBS-modified asphalt-high-viscosity modifier ratio is 86:14, the overall performance of the high-viscosity asphalt is optimal. According to the results of Cantabro and draindown tests, the optimal asphalt-aggregate ratios of PAC-1-I, PAC-1-II, PAC-2-I and PAC-2-II asphalt mixtures are 4.6%, 4.5%, 5.3%, and 5.3%, respectively. The performance of the four asphalt mixtures designed was verified and meets the requirements.

© 2019 Elsevier Ltd. All rights reserved.

1. Introduction

1.1. Background

In order to improve the service life, skid resistance, drainage and noise reduction performances of pavement, a porous ultra-

* Corresponding author.

E-mail address: 101011363@seu.edu.cn (S. Luo).

thin overlay (PUTO), as shown in Fig. 1, has been proposed. PUTO combines the functionality of an ultra-thin overlay and a drainage asphalt mixture. If PUTO is to be applied to actual engineering projects, we should first design a PUTO asphalt mixture that meets the requirements in the laboratory. The design of the PUTO asphalt mixture can be divided into three parts: asphalt binder design, aggregate gradation design and optimal asphalt-aggregate ratio determination.

As an ultra-thin overlay, PUTO has a small aggregate size and low structural strength. Therefore, its asphalt binder needs to have a high bond strength to ensure its performance meets the requirements [1,2]. In addition, PUTO also has a large void ratio, resulting in low strength, poor durability, and diseases such as aggregate peeling and looseness are easily caused [3,4,17]. In order to alleviate these problems, high-viscosity asphalt has been proposed, and the most commonly-used high-viscosity asphalt is thermoplastic styrene (TPS)-modified asphalt [5,6]. Based on the results of these predecessors, asphalt binders suitable for PUTO are proposed in this study.

There is no clear reference to the current research results of PUTO's gradation design. Therefore, we can only design a gradation suitable for PUTO according to the existing gradation design methods. At present, the maximum dense curve theory, particle interference theory and fractal theory are the three most commonly-used gradation design theories [7,8]. The theory of the maximum dense curve was proposed by American scientist W.B. Fuller [9]. This shows that the aggregate has the highest density when it is composed according to the maximum dense curve. However, pavement structure designed based on this theory is prone to high temperature rutting, wave, displacement and other deformations [7,10,11]. According to the particle interference theory, in order to achieve the maximum density, the gap between the particles of the previous stage should be filled by the particles of the next stage, and the remaining spaces are filled by the particles of the next stage. To avoid interference, the particle size used to fill the void should be less than the distance between gaps. The application of fractal theory in asphalt mixtures was developed by Sun et al. [12] after summarizing the preliminary research results obtained in the fields of metal and geotechnical materials. The fractal formula of the gradation aggregate particle size distribution function and the fractal gradation formula of aggregate were derived [13]. According to these three gradation design theories, the following types of aggregate gradation are produced: continu-

ous dense gradation, intermittent gradation, broken gradation and multi-stage embedded compact gradation [10]. For PUTO asphalt mixtures, the void ratio is as high as 20%, and as an ultra-thin overlay, sufficient structural strength is required to resist high-temperature deformation and bear repeated wear of wheels. The PUTO asphalt mixture is a typical skeleton-void structure, which is based on particle interference theory, and its gradation can be designed based on particle interference theory. These gradation types have different gradation design methods, including the Marshall volume design method and the Bailey design method [14,29]. The Marshall volume design method is an asphalt mixture design method commonly used in China. The method considers that the sum of the fine aggregate volume, the mineral powder volume, the asphalt volume, and the void volume is equal to the volume of the main skeleton gap [15,16]. In this way, the skeleton of the coarse aggregate can be fully utilized, and at the same time, fine aggregate can effectively fill the void. The Bailey design method is an asphalt mixture grading design method proposed by Robert D. Bailey in the early 1980s [14]. The breakthrough of this method is to redefine the boundary point of the coarse aggregate, and the nominal maximum particle size of 0.22 times is used as the first control sieve, which is different from the traditional dividing method. By combining these gradation design methods, we hope to design a gradation suitable for PUTO.

After the asphalt binder and gradation design is completed, the optimal asphalt-aggregate ratio needs to be determined to complete the design of the PUTO asphalt mixture. First, the use of asphalt was estimated based on the Technical Specification for Construction of Highway Asphalt Pavement in China (JTG F40-2004) [18]. The optimal asphalt-aggregate ratio is then calculated by the results of the draindown and Cantabro tests to complete the design of the PUTO asphalt mixture.

Based on the above discussion, two high-viscosity modifiers and two blended asphalts were used to prepare the high-viscosity asphalt. Dynamic shear rheology (DSR) tests, 60 °C dynamic viscosity tests, Fourier transform infrared spectroscopy (FTIR) tests and physical properties tests were used to study the modification effect and modification mechanism of high-viscosity asphalt. Then, based on existing gradation design methods, two types of gradation, coarse and fine, were designed for PUTO. In addition, based on the results of the draindown and Cantabro tests, the optimal asphalt-aggregate ratio was determined. Finally, the performance of the designed PUTO asphalt mixture was verified.

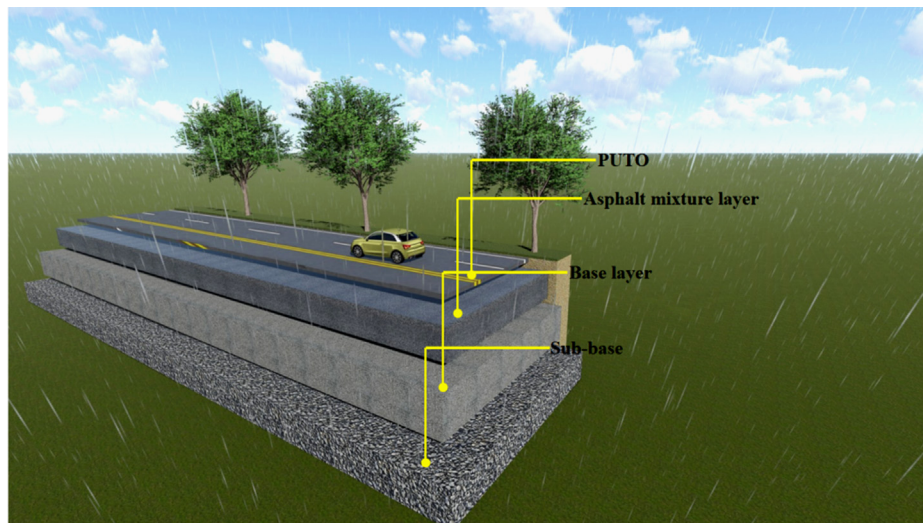


Fig. 1. PUTO in pavement structure.

1.2. Objectives of this study

The main purpose of this study was to design a PUTO asphalt mixture, and the design process can be divided into the following steps:

- 1) Preparation of asphalt binder suitable for PUTO.
- 2) Design of an aggregate gradation that meets the requirements of PUTO.
- 3) Determination of the optimal asphalt-aggregate ratio to complete the design of the PUTO asphalt mixture.
- 4) Verification of the performance of the PUTO asphalt mixture.

Fig. 2 shows the detailed design process for the PUTO asphalt mixture.

2. Materials

2.1. Asphalt

In this research, styrene–butadienestyrene (SBS)-modified asphalt and 70# original asphalt were selected as the blended asphalts, and the test results for the basic physical properties are shown in Tables 1 and 2, according to the Standard Test Method of Bitumen and Bituminous Mixture for Highway Engineering in China (JTG E20-2011) [19].

2.2. Aggregates

2.2.1. Coarse aggregates

PUTO is used as the surface layer of pavement. In addition to skid resistance and drainage functions, it also has direct contact with the wheels and needs to bear a certain load capacity. At the same time, due to its structural characteristic of large pores, the proportion of coarse aggregates is greater than that of fine aggregates, and the selection of coarse aggregates should therefore be strictly monitored. In this research, the hard texture of aggregates was selected, and the basic performance test results are shown in Table 3 according to the Testing Procedures of Aggregate for Highway Engineering in China (JTG E42-2005) [20].

2.2.2. Fine aggregates

Only fine aggregates are used as aggregates for asphalt mixtures, such as AC-5 and SMA-5, which are prone to problems such as rutting and aggregate breakage. However, the surface roughness and angularity of fine aggregates are effective in improving the Marshall stability and rutting resistance of asphalt mixtures. Therefore, some strict requirements on the quality of fine aggregates are given, and the performance test results are shown in Table 4 according to the Testing Procedures of Aggregate for Highway Engineering in China (JTG E42-2005) [20].

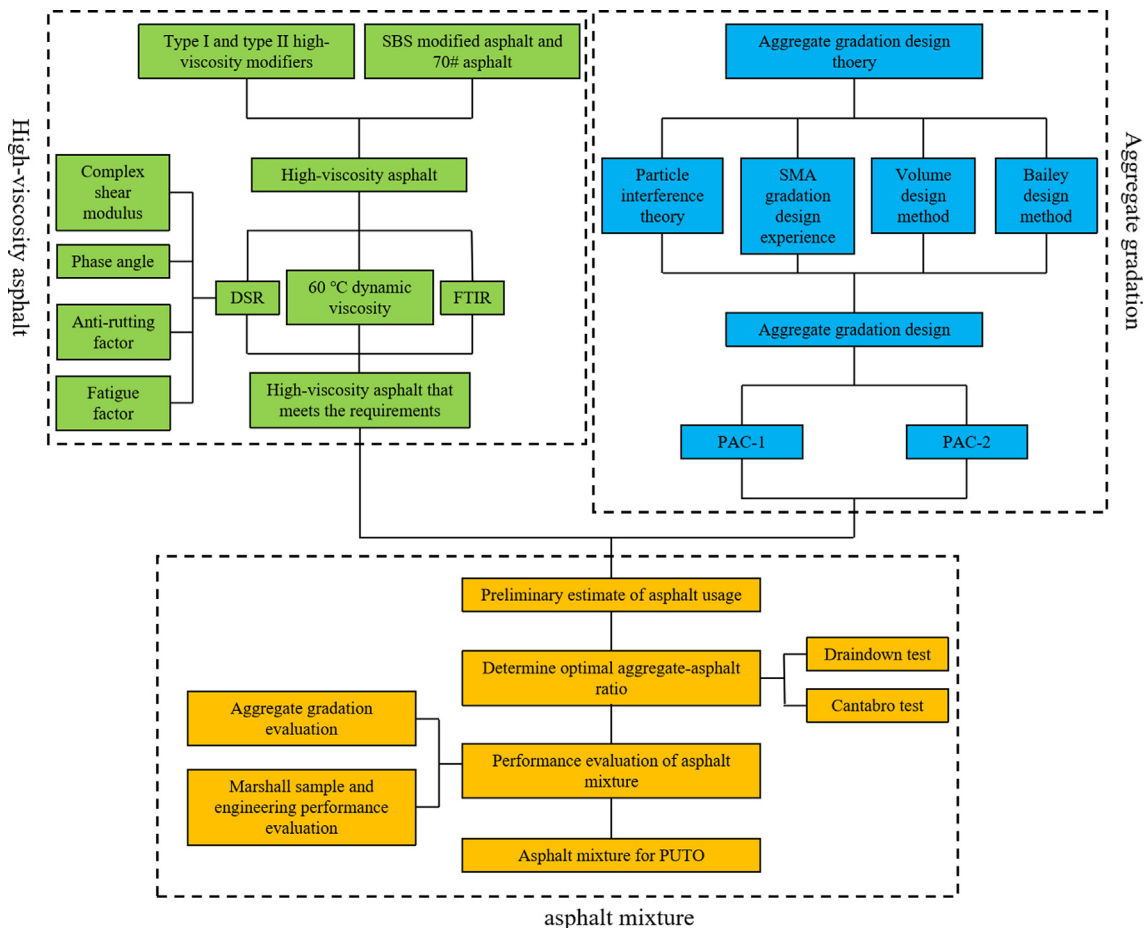


Fig. 2. PUTO asphalt mixture design process.

Table 1
Properties of SBS-modified asphalt.

Test items	Test results	Standard results	Test methods
Penetration (25 °C, 100 g, 5 s) /0.1 mm	68.8	60~80	T 0604-2011
Softening point (TR&B)	64.6	>55 °C	T 0606-2011
Ductility (5 °C, 5 cm/min)/cm	52.8	≥30	T 0605-2011
Penetration index	0.26	≧-0.4	T 0604-2011
Flexible recovery (25 °C)/%	79	≧65	T 0662-2011
Density (25 °C)/g/cm ³	1.079	N/A	T 0603-2011
After TFOT	Mass loss/%	≤±1.0	T 0609-2011
	Penetration ratio (25 °C)/%	≧60	T 0604-2011
	Ductility (5 °C)/cm	≧20	T 0605-2011

Table 2
Properties of 70# original asphalt.

Test items	Test results	Standard results	Test methods
Penetration (25 °C, 100 g, 5 s) /0.1 mm	66.6	60~80	T 0604-2011
Softening point (TR&B)	48.8	>46 °C	T 0606-2011
Ductility (5 °C, 5 cm/min)/cm	21.5	≥20	T 0605-2011
Penetration index	-1.6	-1.5~1.0	T 0604-2011
Flexible recovery (25 °C)/%	1.042	N/A	T 0603-2011
Density (25 °C)/g/cm ³	0.02	≤±0.8	T 0609-2011
After TFOT	Mass loss/%	≥61	T 0604-2011
	Penetration ratio (25 °C)/%	≧6	T 0605-2011
	Ductility (5 °C)/cm	60~80	T 0604-2011

Table 3
Properties of coarse aggregates.

Test items	Test results	Standard results	Test methods
Soft stone content/%	0.6	≤1.0	T0320-2005
Crushed ratio/%	10.5	≤18	T0316-2005
Apparent density/g/cm ³	2.991	≧2.70	T0304-2005
Water absorption rate/%	0.8	≤1.0	T0304-2005
Los Angeles wear loss/%	15	≤20	T0317-2005
Ruggedness/%	3.5	≤8	T0314-2005
Flat and elongated particle content/%	1.4	≤12	T0312-2005
Polished stone value	51	≧42	T0321-2005

2.3. High-viscosity modifiers

In this research, two kinds of commonly-used high-viscosity modifiers were selected as raw materials, which are recorded as Type I high-viscosity modifier and Type II high-viscosity modifier, respectively, as shown in Fig. 3. Both high-viscosity modifiers were sourced from Shanghai, China. The basic properties test results are shown in Table 5.

3. Preparation and performance of high-viscosity asphalt

3.1. Preparation of high-viscosity asphalt

A small high-speed shear meter from PRIMIX Corporation, Japan was used to prepare the high-viscosity asphalt binders. The prepara-

tion process is shown in Fig. 4. 70# original asphalt, SBS-modified asphalt and Type I high-viscosity modifier and Type II high-viscosity modifier were blended to prepare four types of high-viscosity asphalt, which were recorded as 70#-I, 70#-II, SBS-I and SBS-II respectively. In the design of the drainage asphalt mixture, the blending mass ratio of asphalt and high-viscosity modifier is usually set to 88:12 [21]. In this study, 88:12 was used as the median value, and the amount of high-viscosity modifier was increased by ±2 and ±4, respectively. That is, each type of high-viscosity asphalt had a total of five ratios: 84:16, 86: 14, 88:12, 90:10 and 92:8, respectively.

3.2. Dynamic shear rheological (DSR) test

The DSR test was carried out to evaluate the modification effect of the high-viscosity modifier on the two types of asphalt. The DSR test uses the dynamic mechanical analysis method to obtain rheological evaluation indicators, which effectively avoids the shortage of conventional empirical indicators. In this study, the DSR-CV0100 ADS dynamic shear rheometer produced by the American BOHLIN Company was adopted, as shown in Fig. 5. The test was carried out in accordance with the requirements of American Society for Testing Materials (ASTM) standards. The test starting temperature was 58 °C and the termination temperature was 88 °C, measured once every 6 °C [30]. The results of complex shear modulus, phase angle, anti-rutting factor and fatigue factor of asphalt with different high-viscosity modifiers are shown in Figs. 6–9, respectively.

Table 4
Properties of fine aggregates.

Test items	Test results	Standard results	Test methods
Ruggedness/%	2.1	≤3	T0340-2005
Apparent relative density/g/cm ³	2.952	≥2.50	T0328-2005
	2.927		
Sand equivalent/%	71.3	≥60	T0334-2005
Methylene blue value/g/kg	0.8	≤1.5	T0349-2005
Crushed value	6	≤10	T0350-2005
Angularity/%	33	≥30	T0345-2005
Clay content/%	1.8	≤3.0	T0333-2005

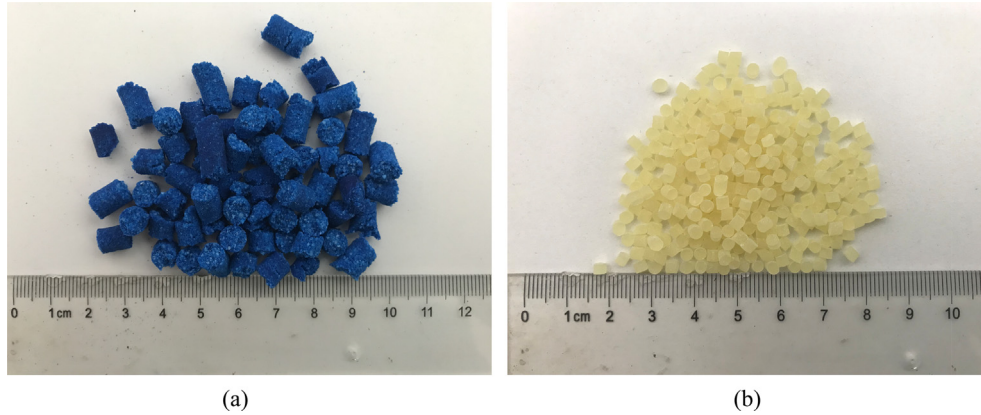


Fig. 3. High-viscosity modifiers: (a) Type I high-viscosity modifier; (b) Type II high-viscosity modifier.

Table 5
Properties of high-viscosity modifiers.

Test items	Test results		Standard results	Test methods
	Type I high-viscosity modifier	Type II high-viscosity modifier		
Exterior	Blue particles, evenly dispersed	Yellow particles, evenly dispersed	Granular, evenly dispersed	Visual inspection
Individual particle mass/g	0.14	0.05	≤0.5	Weighing
Ash/%	0.35	0.4	≤1.0	T 0614-2011
Dry mix dispersability	A little residue	No residue	No residue	Dry mix

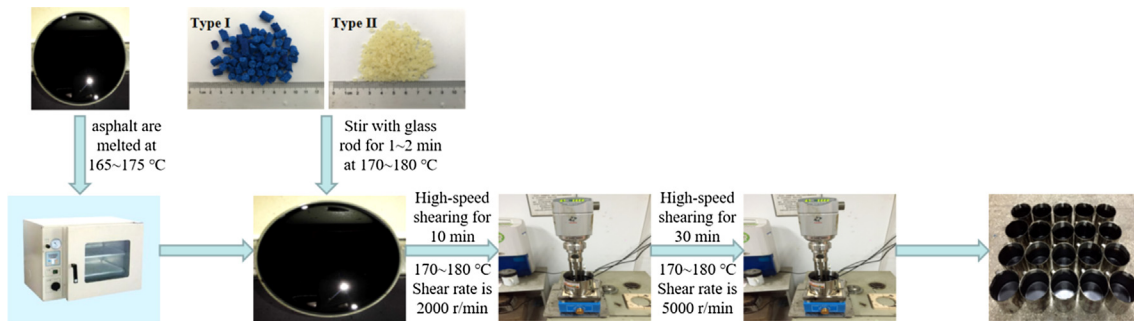


Fig. 4. Preparation process of high-viscosity modifier-modified asphalt.



Fig. 5. Dynamic shear rheometer.

3.2.1. Complex shear modulus

Fig. 6 shows that the complex shear modulus (G^*) of the four high-viscosity asphalts is consistent with the temperature. As the temperature gradually increases, G^* gradually decreases and the G^* of different modifier types and contents tend to be equal. For

the same blended asphalt, as the amount of high-viscosity modifier increases, G^* also increases. This can be explained by the fact that a high-viscosity modifier forms a three-dimensional elastic network structure between polymerization and asphalt molecules, thereby hindering the movement between asphalt molecules, resulting in a decrease in the flow properties of asphalt and an enhanced resistance to deformation.

Comparing Fig. 6(a) and (b) or Fig. 6(c) and (d), it is clear that the G^* of asphalt with Type II high-viscosity modifier is larger than that of asphalt with Type I high-viscosity modifier when the blended asphalt and the testing temperature are the same. This indicates that the network structure formed between Type II high-viscosity modifier and asphalt is more stable. A comparison of Fig. 6(a) and (c) or Fig. 6(b) and 6(d) reveals that when the type of high-viscosity modifier and the test temperature are the same, the G^* of SBS- modified asphalt used as the blended asphalt is larger than the G^* obtained for the 70# original asphalt used as the blended asphalt. This is because the SBS-modified asphalt itself contains SBS modifier, and its internal polystyrene molecules improve the tensile strength of asphalt under high-temperature conditions.

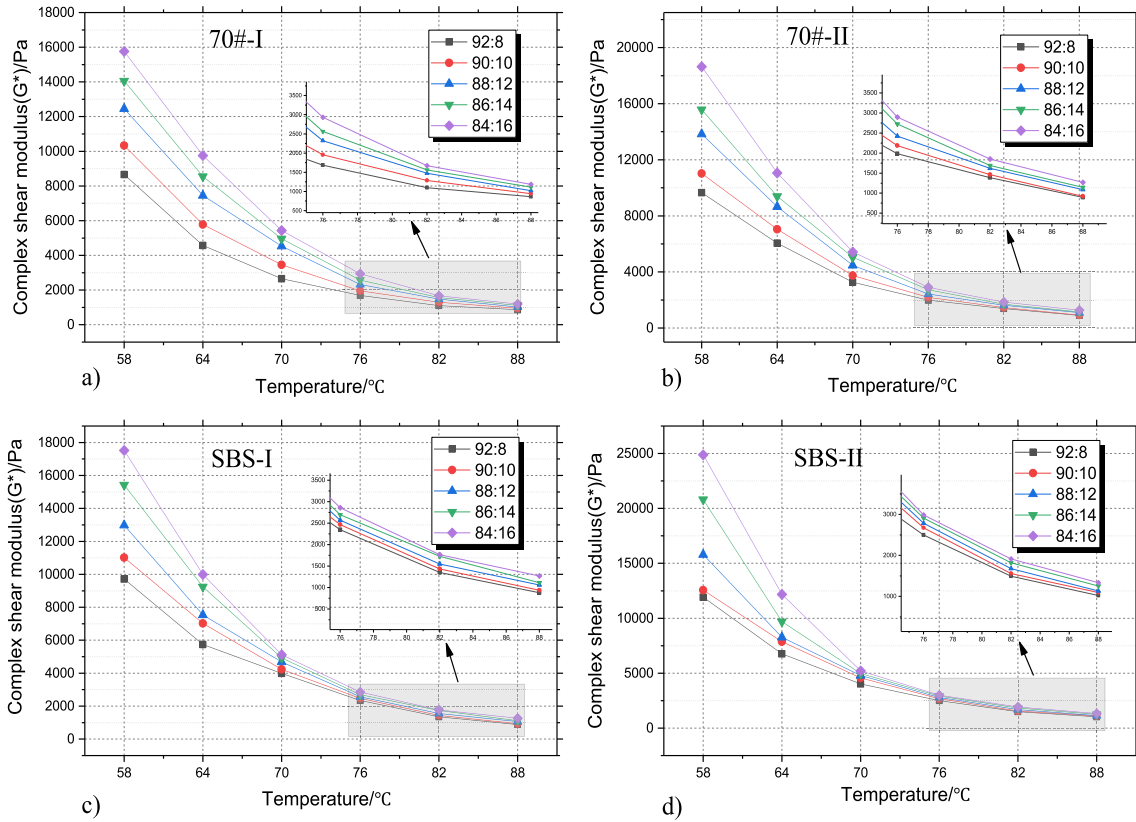


Fig. 6. Curves of G^* with temperature for different high-viscosity modifier contents.

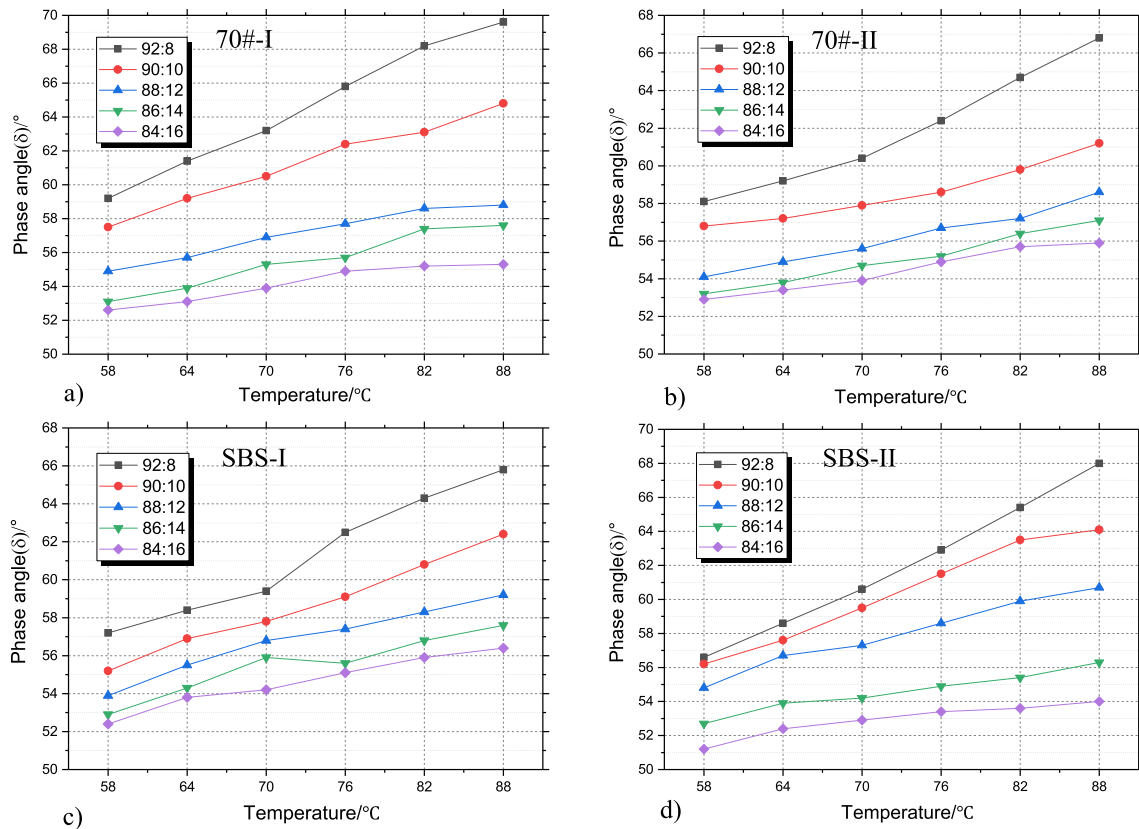


Fig. 7. Curves of phase angle with temperature for different high-viscosity modifier contents.

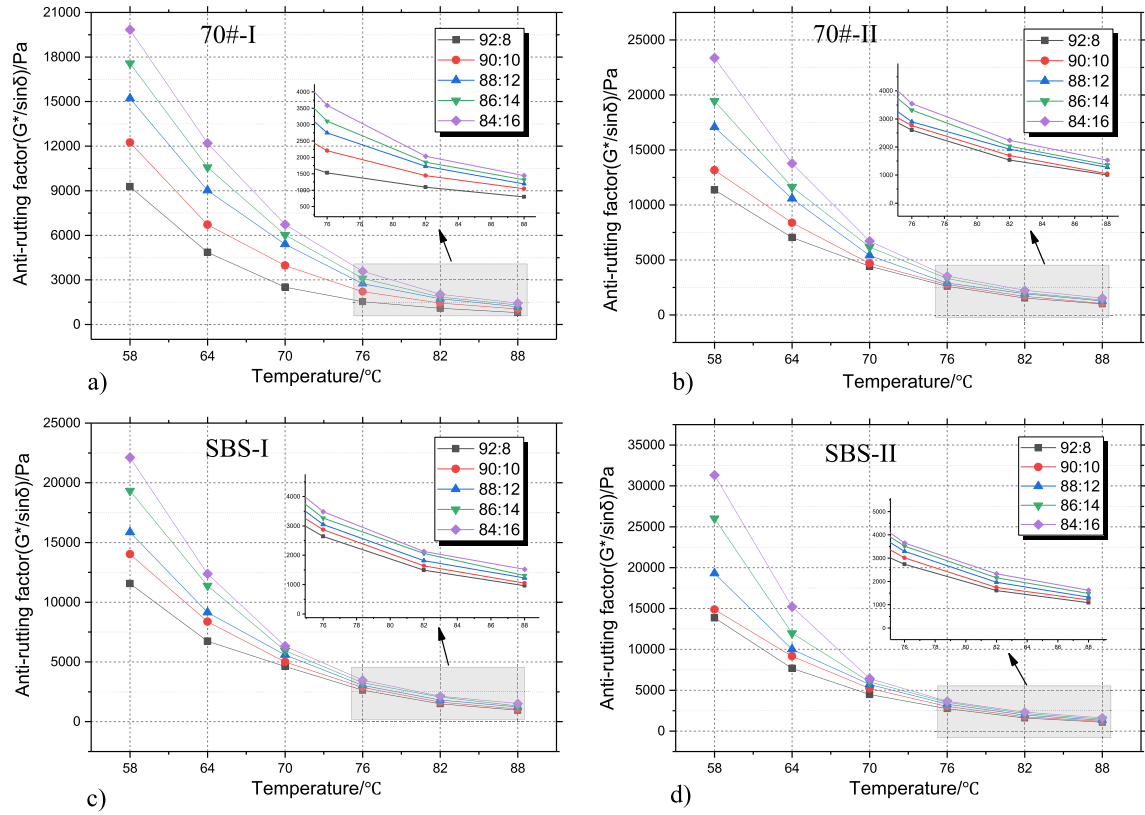


Fig. 8. Curves of anti-rutting factor with temperature for different high-viscosity modifier contents.

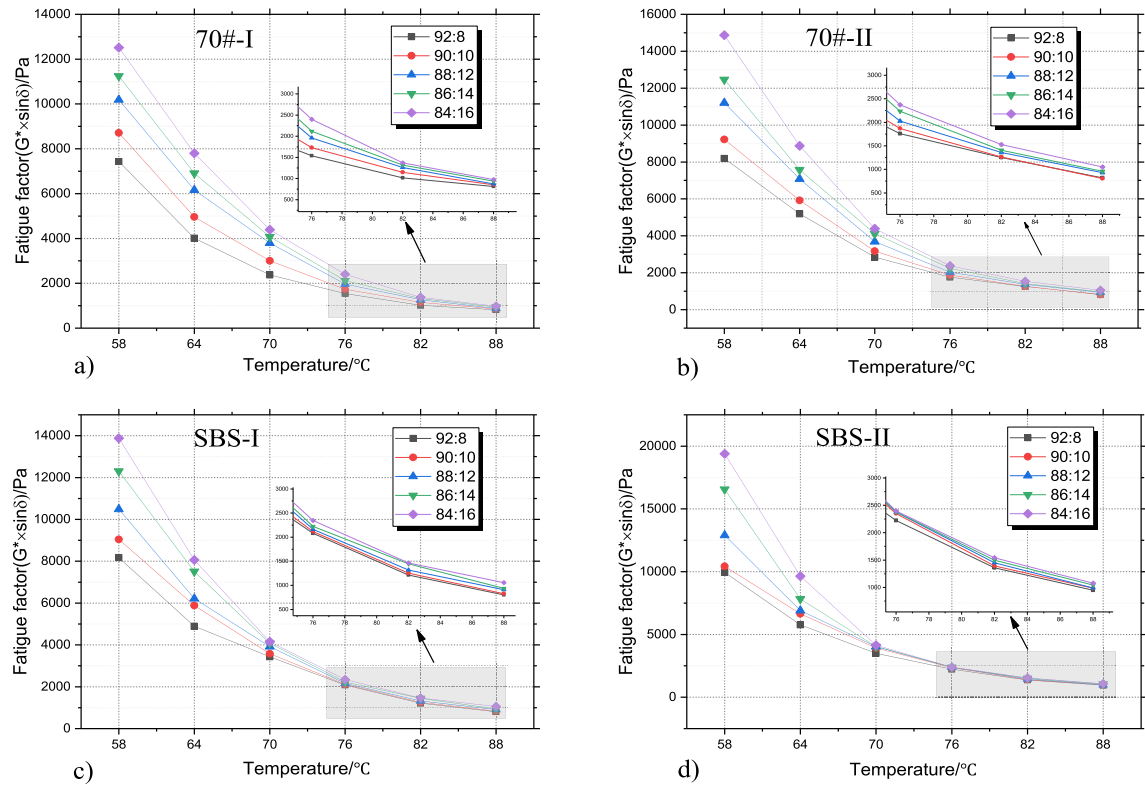


Fig. 9. Curves of fatigue factor with temperature for different high-viscosity modifier contents.

3.2.2. Phase angle

Fig. 7 indicates that the phase angles (δ) of the four high-viscosity asphalts increase with increasing temperature. This is because the proportion of the viscoelastic component in the asphalt changes when the temperature changes. When the temperature rises, the proportion of the viscous component is increased, that is, the unrecoverable part of deformation increases, and permanent deformation is more likely to occur. Further observations reveal that the spacings between the curves for different high-viscosity modifier contents are not equal, and SBS-II asphalt has the largest reduction in phase angles between 88:12 and 86:14. 70#-I asphalt and 70#-II asphalt have the largest reduction in phase angle between 90:10 and 88:12, while SBS-I asphalt has no obvious regularity.

3.2.3. Anti-rutting factor

Fig. 8 shows that the anti-rutting factors of the four high-viscosity asphalts decrease with increasing temperature. For any kind of high-viscosity asphalt, with the increase of the content of high-viscosity modifier, the anti-rutting factor gradually increases, but the increment is slightly different. Taking the test temperature of 58 °C as an example, the increased maximum values of the rutting factors of four high-viscosity asphalts appear at 88:12, 88:12, 86:14 and 86:14, respectively, for the five contents. They increased by 2969 Pa, 2812 Pa, 3484 Pa and 6727 Pa, respectively. This indicates that the four high-viscosity asphalts have the most obvious effect on the improvement of the high-temperature stability for contents of 88:12, 88:12, 86:14 and 86:14. When the content of high viscosity modifier is further increased, the effect of improving the resistance to rutting deformation under high temperature conditions is limited, and these four contents can therefore be considered as optimum contents.

3.2.4. Fatigue factor

According to Fig. 9, for any high-viscosity asphalt, its fatigue factor decreases with increasing temperature or decreasing amount of high-viscosity modifier. This can be understood as the fatigue factor ($G^* \times \sin \delta$) obtained by multiplying G^* and $\sin \delta$. G^* decreases rapidly with increasing temperature. Although δ increases with temperature, since the increase is much smaller than the decrease of G^* , the overall trend of $G^* \times \sin \delta$ is still decreasing. This indicates that increasing the temperature or reducing the amount of high-viscosity modifier is beneficial for the improvement of the fatigue resistance of asphalt, which is the opposite of the test results for the anti-rutting factor. Therefore, the optimum amount of high-viscosity modifier needs to be determined in consideration of most properties of high-viscosity asphalt.

3.3. 60 °C dynamic viscosity test

As a basic performance index of asphalt, viscosity reflects the frictional resistance between asphalt molecules, which directly affects the water sensitivity and flaking resistance of the asphalt mixture [22]. PUTO has a typical open gradation structure, which has a void ratio of up to about 20%, and at the same time, because its thickness is only 1.5~2.5 cm, it is easy to loosely peel off under driving conditions. Therefore, in order to ensure the bonding ability between asphalt and aggregates, and prolong the service life of PUTO, high-viscosity asphalt is used as a binder. In this study, the vacuum decompression capillary method was used to detect the 60 °C dynamic viscosity of four types of high-viscosity asphalt, and their changes of viscosity were analyzed. The results are shown in Fig. 10.

As Fig. 10 shows, the dynamic viscosities of the four high-viscosity asphalts increase with the increase of high-viscosity mod-

ifier content. When the type of modifier is the same, the dynamic viscosity of SBS- modified asphalt as the blended asphalt is greater than that of 70# asphalt. When the blended asphalt is the same, the improvement of the dynamic viscosity of asphalt with Type II high-viscosity modifier is better than that of asphalt with Type I high-viscosity modifier. The Japanese road specification clearly states that when asphalt is used for the drainage of asphalt pavement, its 60 °C dynamic viscosity should be no less than 20,000 Pa·s [23]. Due to the serious overload phenomenon of asphalt pavement in China, and the small particle size and thin thickness of PUTO, the requirement of 20,000 Pa·s is far from meeting the needs of pavement. Therefore, this study proposes a requirement of 60 °C dynamic viscosity for high-viscosity asphalt exceeding 100,000 Pa·s. The asphalt and its content which satisfy the technical requirements are 1. SBS-I high-viscosity asphalt with high-viscosity modifier contents of 14% and 16%, respectively; 2. SBS-II high-viscosity asphalt with high-viscosity modifier contents of 14% and 16%, respectively.

3.4. Fourier transform infrared (FTIR) spectroscopy test

In order to reveal the modification mechanism of high-viscosity asphalt, FTIR was used to test 70# asphalt, SBS-modified asphalt, Type I high-viscosity modifier and Type II high-viscosity modifier, and analyze their characteristic peaks. On this basis, the infrared spectrum of high-viscosity asphalt with different high-viscosity modifier contents was tested, and the variation of characteristic peaks with the content of high-viscosity modifier was analyzed. The infrared spectra of the raw materials of the four high-viscosity asphalts are shown in Fig. 11.

It can be seen from Fig. 11(a) that 70# asphalt has obvious absorption peaks at wavenumbers of 2926 cm^{-1} , 1600 cm^{-1} , 1376 cm^{-1} and 813 cm^{-1} , which is due to $-\text{CH}_2-$, $\text{C}=\text{C}$, $-\text{CH}_3-$, and $\text{C}-\text{H}$ molecules constantly stretching and shaking or rocking. Based on the results of Pu et al. [24], it is known that the absorption peak of original asphalt at 813 cm^{-1} is relatively stable and can be used as a reference characteristic absorption peak in quantitative analysis. SBS-modified asphalt is obtained by blending original asphalt and SBS modifier. Therefore, in addition to the characteristic absorption peak of the original asphalt in Fig. 11(b), a new characteristic peak is generated at 966 cm^{-1} , which is caused by the bending vibration of $\text{C}-\text{H}$ at $\text{C}=\text{C}$ in SBS.

The composition of the two high-viscosity modifiers is complex, including thermoplastic rubbers, tackifiers, plasticizers, coupling agents, and colorants. Their infrared spectra are shown in (c) and (d) of Fig. 11. Of these, thermoplastic rubber is the main compo-

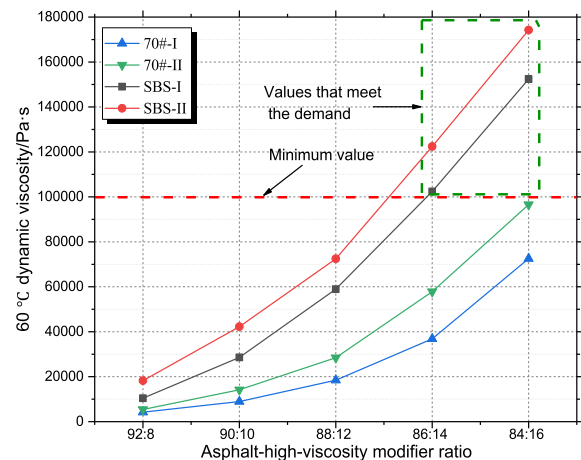


Fig. 10. 60 °C dynamic viscosity test results of high-viscosity asphalt.

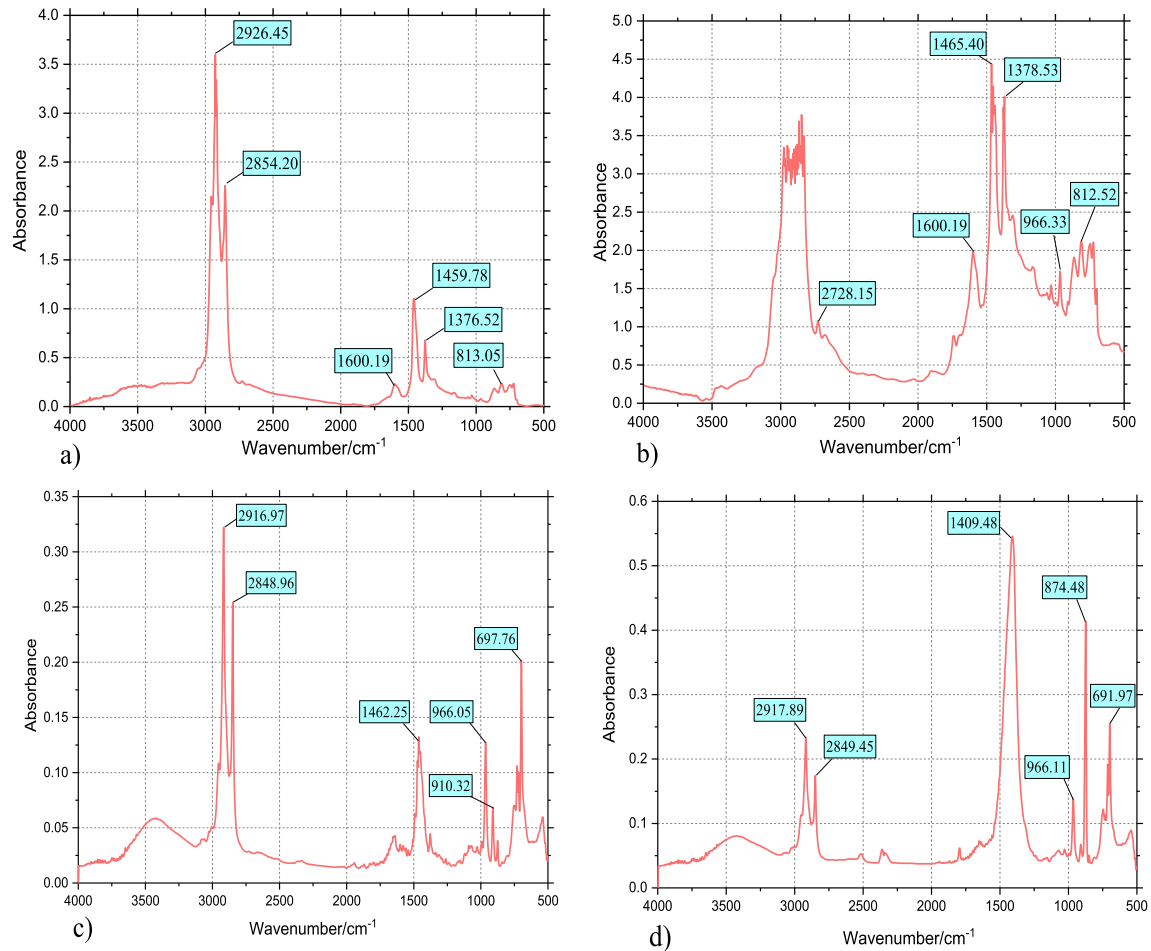


Fig. 11. Infrared spectrum of four high-viscosity asphalts raw materials: (a) 70#; (b) SBS modified asphalt; (c) Type I modifier; (d) Type II modifier.

ment of high-viscosity modifier, which is obtained by polymerization of styrene and butadiene, similar to the composition of SBS modifier. Therefore, the Type I high-viscosity modifier and the Type II high-viscosity modifier also have characteristic absorption peaks at 966 cm^{-1} . When the high-viscosity modifier is mixed with asphalt at a high temperature, swelling occurs, and the light components in asphalt are absorbed, so that the heavy components are increased, and the viscosity and softening point of asphalt are improved. At the same time as the modifier swells, polymer such as polystyrene gradually diffuses into the asphalt and physically cross-links with other components to form an elastic three-dimensional polymer network structure, thereby damping the flow of asphalt to achieve the effect of thickening. This indicates that the main component of the high-viscosity modifier for modifying the original asphalt is thermoplastic rubber, which forms a polymer network structure between the polymer in the high-viscosity modifier and the asphalt component, which is reflected in the infrared spectrum. That is, there is a significant characteristic absorption peak at 966 cm^{-1} in the fingerprint vibration spectrum region ($1500\text{--}600\text{ cm}^{-1}$).

3.5. Physical properties

Penetration, softening point and ductility are commonly-used indicators for the evaluation of the basic properties of asphalt. Their numerical values are closely related to the performance of asphalt. Since the results of Section 3.3 show that only SBS-I and SBS-II high-viscosity asphalts meet the requirements, this section

evaluates only these two kinds of asphalt, and recommends the optimal high-viscosity modifier amount.

Fig. 12 shows that as the amount of high-viscosity modifier increases, the ductility and softening point of the two high-viscosity asphalts gradually increase, and the penetration gradually decreases. When the amount of high-viscosity modifier is increased from 8% to 14%, the penetration decreases linearly, and when its amount reaches 14%, the penetration decreases slowly, and the growth rate of ductility and the softening point also slow. Further comparison of the results of the three indices of SBS-I and SBS-II high-viscosity asphalts shows that the penetration of SBS-II high-viscosity asphalt is less than that of SBS-I high-viscosity asphalt, indicating that the consistency of SBS-II high-viscosity asphalt is greater. This is consistent with the test results of the $60\text{ }^{\circ}\text{C}$ dynamic viscosity. On the other hand, the ductility and softening point of SBS-II high-viscosity asphalt are higher than those of SBS-I high-viscosity asphalt, indicating that the high temperature performance and low temperature performance of SBS-II high-viscosity asphalt are slightly better than those of SBS-I high-viscosity asphalt. Considering the total economic cost, when the blending ratio of SBS-modified asphalt and high-viscosity modifier is 86:14, the overall performance of high-viscosity asphalt is optimal.

4. Aggregate gradation design

Since the recommended gradation range of PUTO is not given in the Technical Specification for Construction of Highway Asphalt

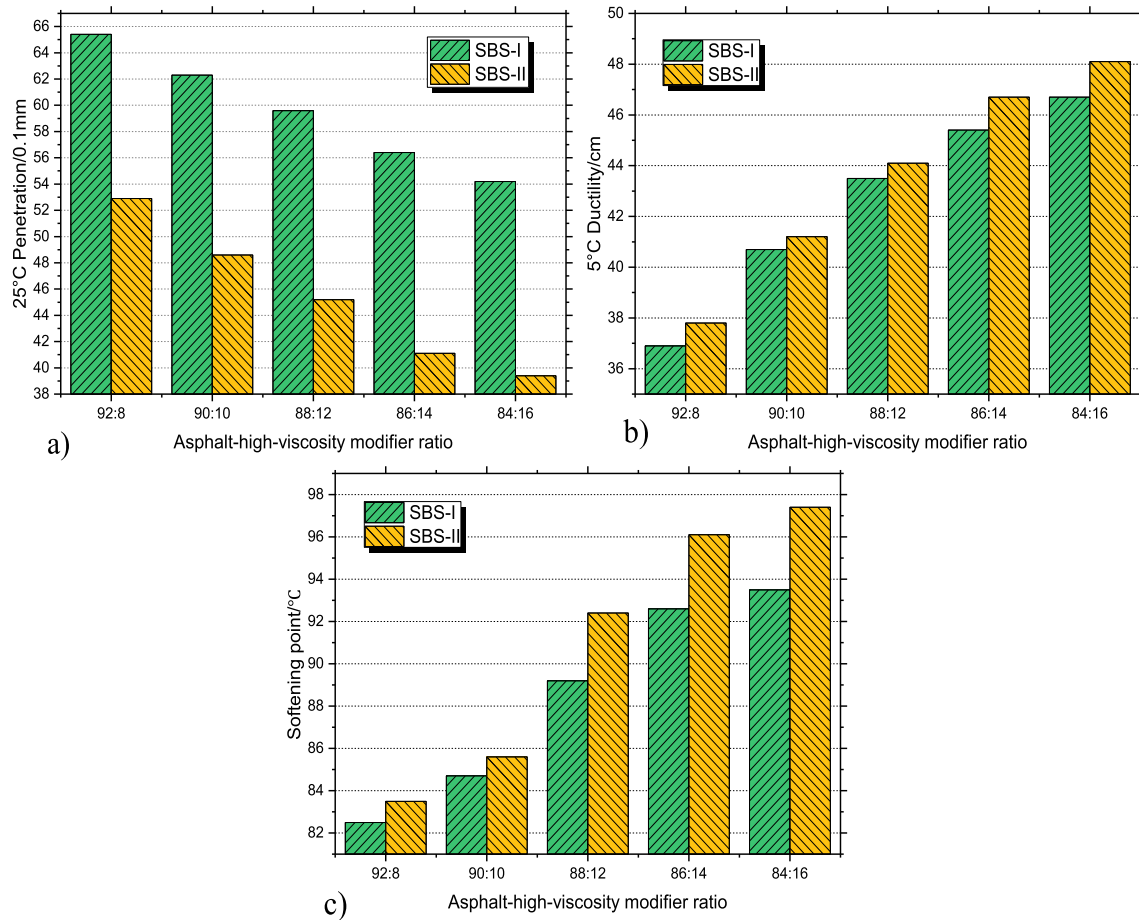


Fig. 12. Physical properties of high-viscosity asphalt.

Pavement in China (JTG F40-2004) [18], this study designed the gradation composition of PUTO according to existing theory. Based on the particle interference theory proposed by Weymouth [8], SMA gradation design method [25], the volume design method and the Bailey design method [14], the gradation composition of PUTO is determined to ensure that it meets engineering requirements and has a void ratio more than 20%. The design steps for the gradation composition of PUTO are as follows:

- 1) Preset parameters, including the design density, the volume composition, and the pass rate of the 0.075 mm sieve of aggregate are determined. The design density of coarse aggregate = bulk density of coarse aggregate × expected percentage of bulk density. In order to ensure the formation of stone-stone contact between the coarse aggregate particles, the expected percentage of bulk density is generally controlled at between 95% and 105% [10]. The design density of fine aggregate is taken from compact density to ensure that the fine aggregate structure reaches or approaches its maximum strength.
- 2) The mass of the coarse aggregate per unit volume is determined.
- 3) The voids in coarse aggregate (VCA) under the design density are calculated. $VCA = (1 - \text{design density}/\text{bulk volume density}) \times \text{coarse aggregate volume ratio}$.
- 4) The reserved void ratio is determined. According to the volume design method, VCA consists of the volume of voids, fine aggregate, asphalt and mineral filler. Since the volume

- occupied by fine aggregate and mineral filler is considered in steps (5) and (8), respectively, the reserved void ratio mainly includes the target void ratio and the asphalt volume.
- 5) According to the VCA and the reserved void ratio, the fine aggregate volume ratio is determined, and the fine aggregate mass per unit volume is calculated.
- 6) The initial mass percentage of the coarse and fine aggregates is calculated based on the coarse and fine aggregate mass per unit volume.
- 7) According to the Bailey design method [14], the 0.22 times nominal maximum particle size (NMPS) is used as the demarcation point between coarse and fine aggregates. The aggregate mass ratio is recalibrated by considering the aggregate below the demarcation point of the coarse aggregate and the aggregate above the demarcation point of the fine aggregate.
- 8) The mass ratios of the aggregate below 0.075 mm sieve in each type of aggregate and mineral filler are calculated, and the mass percentages of the coarse and fine aggregates are corrected.
- 9) The final mass ratios of coarse aggregate, fine aggregate, and mineral filler are determined, and the gradation composition is determined by considering their respective screening results.

In order to study the influence of different gradation compositions on PUTO performance, two nominal maximum particle sizes of 9.5 mm and 4.75 mm were selected for gradation design. Two

Table 6
Aggregate screening results.

Aggregate type	Screening pass rate/%							
	9.5 mm	4.75 mm	2.36 mm	1.18	0.6 mm	0.3 mm	0.15 mm	0.075 mm
CA-1	100.0	0.4	0.1	0.0	0.0	0.0	0.0	0.0
CA-2	100.0	100.0	0.0	0.0	0.0	0.0	0.0	0.0
FA-1	100.0	100.0	39.7	3.1	0.5	0.4	0.0	0.0
FA-2	100.0	100.0	100.0	71.0	29.3	10.5	5.3	1.7
MF	100.0	100.0	100.0	100.0	100.0	90.7	76.0	59.6

Table 7
Aggregate density test results.

Test item	Aggregate type				
	CA-1	CA-2	FA-1	FA-2	MF
Apparent density/g/cm ³	2.991	2.954	2.952	2.927	2.67
Bulk volume density/g/cm ³	2.922	2.893	N/A	N/A	2.67
Bulk density/g/cm ³	1.610	1.602	N/A	N/A	N/A
Dry density/g/cm ³	1.714	1.702	1.732	1.746	N/A

Table 8
PAC-I and PAC-II gradations.

Gradation type	Mass percentage of aggregates through each sieve/%							
	9.5 mm	4.75 mm	2.36 mm	1.18 mm	0.6 mm	0.3 mm	0.15 mm	0.075 mm
PAC-1	100.0	17.7	11.0	7.0	6.8	6.1	5.1	4.0
PAC-II	100.0	91.3	13.9	11.7	8.6	6.6	5.3	3.9

coarse aggregates (CA-1 and CA-2), two fine aggregates (FA-1 and FA-2) and one mineral filler (MF) were used. The screening results and densities of the various aggregates are summarized in Tables 6 and 7, respectively.

According to the above steps and aggregate parameters, the gradation compositions of PUTO with nominal maximum particle sizes of 9.5 mm and 4.75 mm were designed, respectively. The results are shown in Table 8.

5. Determine optimal aggregate-asphalt ratio

According to the Technical Specifications for Highway Asphalt Pavement Construction (JTG F40-2004) [18] and the calculation method of the conventional drainage asphalt mixture, the initial asphalt-aggregate ratio of the PAC-1 asphalt mixture was estimated to be 4.7%, and the initial asphalt-aggregate ratio of the PAC-2 asphalt mixture was 5.4%. These two values were taken as the median value of $P_a \pm 0.5\%$ and $P_a \pm 1.0\%$. Therefore, the predicted asphalt-aggregate ratio of the PAC-1 asphalt mixture was 3.7%, 4.2%, 4.7%, 5.2%, and 5.7%, respectively, and the predicted asphalt-aggregate ratio of the PAC-2 asphalt mixture was 4.4%, 4.9%, 5.4%, 5.9%, and 6.4%, respectively. Since the initial asphalt-aggregate ratio is related only to aggregate, the initial asphalt-aggregate ratio of the PAC-1-I and PAC-1-II mixtures is the same, and the initial asphalt-aggregate ratio of the PAC-2-I and PAC-2-II is the same.

The draindown and Cantabro tests were designed by the Scherrenburg Institute of Germany and the University of Cantabro, Spain, to determine the reasonable amount of asphalt in asphalt mixture. Therefore, in this study, it was decided to use these two tests to determine the optimal asphalt-aggregate ratio for PUTO. The test results of the draindown test and the Cantabro test are summarized in Fig. 13. Based on Fig. 13, it can be concluded that the range of the asphalt-aggregate ratios of PAC-1-I, PAC-1-II, PAC-2-I and PAC-2-II asphalt mixtures is 4.36%~4.97%, 4.27%~

4.96%, 5.12%~5.31% and 5.01%~5.3%, respectively. According to the specification requirements [18], the draindown loss does not exceed 0.3% and the Cantabro loss does not exceed 20% of drainage asphalt mixture. Therefore, the asphalt-aggregate ratio ranges of the PAC-1-I and PAC-1-II asphalt mixtures can be further reduced to 4.36%~4.6% and 4.27%~4.51%. In order to maximize the engineering performance and service life of PUTO, the maximum asphalt content of the asphalt-aggregate ratio within a reasonable range is selected. Therefore, the optimal asphalt-aggregate ratio of the PAC-1-I and PAC-1-II asphalt mixtures can be determined to be 4.6% and 4.5%, respectively. Similarly, the optimal asphalt-aggregate ratio of the PAC-2-I and PAC-2-II asphalt mixtures can also be determined to be 5.3% and 5.3%, respectively.

It is obvious that the optimal asphalt-aggregate ratio of the asphalt mixture with PAC-1 gradation is smaller than that of the asphalt mixture with PAC-2 gradation. This is mainly because PAC-2 is a fine gradation, and since the proportion of fine aggregate in the mixture is larger, the specific surface area of the aggregate is larger than that of PAC-1. Therefore, if the two gradation asphalt mixtures are to achieve the same asphalt film thickness, the content of asphalt in the PAC-2 asphalt mixture needs to be greater.

6. Performance evaluation of asphalt mixture

6.1. Aggregate gradation evaluation

Whether the designed aggregate grading can meet the requirements requires some methods of evaluation. In the Bailey design method, the coarse aggregate (CA) ratio, fine aggregate coarse (FA_c) ratio and fine aggregate (FA_r) ratio are evaluated for design gradation [26]. However, these three parameters are for a dense grade asphalt mixture, and whether they are suitable for an open-grade asphalt mixture remains to be further verified and discussed.

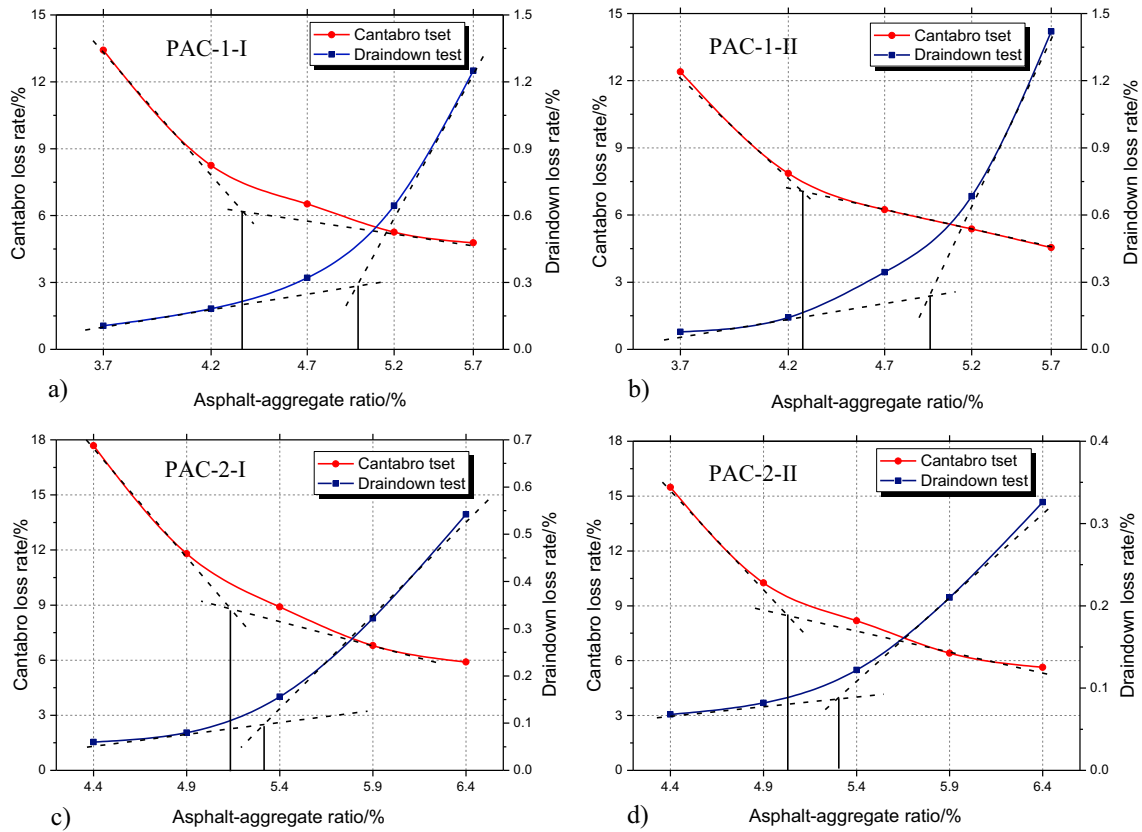


Fig. 13. Draindown and Cantabro test results.

Based on the above discussion, two other evaluation indicators were used to test the design gradation of PUTO in this study. First, according to the evaluation method of the coarse aggregate skeleton in SMA, the VCA_{DRC} of pure coarse aggregate under dry tamping conditions needs to be larger than the VCA_{mix} of coarse aggregate in the asphalt mixture under compaction conditions, otherwise the coarse aggregates do not form a skeleton structure [27]. Second, the skeleton and skeleton contact (SSC) is used to evaluate the degree of mutual contact of the coarse aggregates in a drainage asphalt mixture. When the SSC is >90%, the coarse aggregate in the mixture is considered to form a skeleton structure [28].

The calculation formula for VCA_{mix} is as follows:

$$VCA_{mix} = \left(1 - \frac{\gamma_f}{\gamma_{CA}} \times P_{CA}\right) \times 100 \quad (1)$$

where, γ_f is the gross bulk relative density of the asphalt mixture sample, determined by the surface dry method; γ_{CA} is the average gross bulk relative density of the coarse aggregate skeleton, calculated according to Eq. (2); P_{CA} is the mass ratio of the coarse aggregate in the asphalt mixture, in %.

The formula for γ_{CA} is as follows:

$$\gamma_{CA} = \frac{P_1 + P_2 + \dots + P_n}{\frac{P_1}{\gamma_1} + \frac{P_2}{\gamma_2} + \dots + \frac{P_n}{\gamma_n}} \quad (2)$$

where, P_1, P_2, \dots, P_n are mass percentages of aggregates of different sizes in coarse aggregate respectively occupying all aggregates, in %; $\gamma_1, \gamma_2, \dots, \gamma_n$ are the gross bulk relative densities of the various coarse aggregates.

The calculation formula for VCA_{DRC} is as follows:

$$VCA_{DRC} = \left(1 - \frac{\rho}{\rho_{CA}}\right) \times 100 \quad (3)$$

where, ρ is the dry tamping density of the coarse aggregate, in g/cm^3 ; ρ_{CA} is the bulk volume density of the coarse aggregate, in g/cm^3 .

The calculation formula for SSC is as follows:

$$SSC = \frac{\rho_C}{\rho} \times 100 \quad (4)$$

where, ρ_C is the coarse aggregate density, calculated according to Eq. (5), in g/cm^3 .

The calculation formula for ρ_C is as follows:

$$\rho_C = \frac{\rho_f \times P_{CA}}{100} \quad (5)$$

where, ρ_f is the bulk volume density of the asphalt mixture sample, in g/cm^3 .

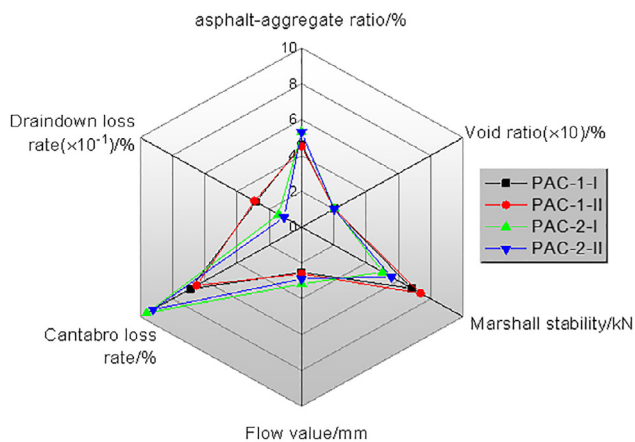
The Marshall samples were formed at the optimal asphalt-aggregate ratio, and its various index parameters were measured and the results are summarized in Table 9. Table 9 shows that the VCA_{mix} of the four asphalt mixtures are smaller than their VCA_{DRC} , and their SSCs are all greater than 90%, which indicates that for both the PAC-1 gradation and the PAC-2 gradation, the internal coarse aggregates form a good skeleton embedded structure, which is very important for the performance of the asphalt mixture.

6.2. Marshall sample performance evaluation

Although the material composition of PUTO has been designed, it is still necessary to verify whether its basic performance meets the requirements. Therefore, the Marshall samples of the four asphalt mixtures were formed at the optimal asphalt-aggregate ratio, and the volume index and Marshall stability were tested. At the same time, draindown and Cantabro tests were carried out, and their basic properties were comprehensively evaluated.

Table 9
Marshall sample parameters.

Test item Asphalt mixture type	PAC-1-I	PAC-1-II	PAC-2-I	PAC-2-II
ρ_f /g/cm ³	2.135	2.126	2.078	2.092
γ_f	2.135	2.126	2.078	2.092
γ_{CA}	2.922	2.922	2.896	2.896
P_{CA} /%	85.1	85.2	83.9	83.9
ρ /g/cm ³	1.729	1.729	1.732	1.732
ρ_{CA} /g/cm ³	2.904	2.904	2.891	2.891
ρ_{cl} /g/cm ³	1.817	1.811	1.743	1.755
VCA_{mix} /%	37.8	38.0	39.8	39.4
VCA_{DRC} /%	40.5	40.5	40.1	40.1
SSC/%	105.08	104.74	100.64	101.33

**Fig. 14.** Performance evaluation results of four asphalt mixtures.

The results are shown in Fig. 14. It can be seen from Fig. 14 that the Marshall stability, flow value, Cantabro loss and draindown loss of the four asphalt mixtures meet the requirements of the specification [18]. In particular, for the porous drainage asphalt mixture, its void ratio generally reaches 18~25% to ensure its functional characteristics including drainage, skid resistance and noise reduction. As Fig. 14 shows, since the void ratios of the four asphalt mixtures all reach 20%, their functional characteristics are guaranteed. Further observation of Fig. 14 shows that the draindown loss rate and the Marshall stability of the PCA-1 asphalt mixture are larger than those of the PAC-2 asphalt mixture, and the asphalt-aggregate ratio, Cantabro loss rate and flow value are smaller than those of the PAC-2 asphalt mixture.

6.3. Engineering performance evaluation

The results of the PUTO engineering performance evaluation are summarized in Table 10. These results indicate that PUTO's engineering performances meet requirements and even some performances exceed expectations. This also proves that the design

Table 10
Engineering performance of PUTO [17].

Test item Asphalt mixture type	PAC-1-I	PAC-1-II	PAC-2-I	PAC-2-II
Dynamic stability/times/mm	8210	8400	856	1438
Bending strain/ $\mu\epsilon$	2822	2896	2532	2678
Splitting tensile strength ratio/%	83.39	84.33	87.52	88.89
Water permeability coefficients/mL/min	7273	7273	6857	6316
Macrostructure depth/mm	0.82	0.85	0.71	0.71
Noise level/dB	76.4	76.7	74.7	74.3

process and method of the asphalt mixture adopted in this study is reasonable. Finally, after considering all performances, the recommended optimal PUTO asphalt mixture type is PAC-1-II.

7. Conclusions

In this study, a porous ultra-thin overlay (PUTO) is proposed as a sustainable and environmentally-friendly asphalt pavement maintenance technology. In order to design the PUTO asphalt mixture, two high-viscosity modifiers and two blended asphalts were used to prepare the high-viscosity asphalt. Dynamic shear rheology (DSR) tests, 60 °C dynamic viscosity tests, Fourier transform infrared spectroscopy (FTIR) tests and physical property tests were used to study the modification effect and modification mechanism of high-viscosity asphalt. Next, based on existing gradation design methods, two types of gradation, coarse and fine, were designed for PUTO. In addition, based on the results of draindown and Cantabro tests, the optimal asphalt-aggregate ratio was determined. Finally, the performance of the designed PUTO asphalt mixture was verified. Based on the results and discussion, the conclusions are as follows:

- 1) With the increase of the amount of high-viscosity modifier, the complex shear modulus and anti-rutting factor of the four kinds of high-viscosity asphalt gradually increased, while their phase angle gradually decreased. SBS-I and SBS-II high-viscosity asphalts have the largest growth rate when the high-viscosity-asphalt ratio is 86:14, and 70#-I and 70#-II high-viscosity asphalts have the largest growth rate when the high-viscosity-asphalt ratio is 88:12.
- 2) In order to meet the requirements for the use of PUTO, the 60 °C dynamic viscosity of high-viscosity asphalt is required to exceed 100,000 Pa·s. The high-viscosity asphalt which satisfies this specification is SBS-I (high-viscosity modifier contents of 14% and 16%) and SBS-II (high-viscosity modifier contents of 14% and 16%).
- 3) The main component of the high-viscosity modifier for the modification of the original asphalt is thermoplastic rubber, which forms a polymer network structure between the polymer in the high-viscosity modifier and the asphalt compo-

ment, which is reflected in the infrared spectrum. That is, there is a significant characteristic absorption peak at 966 cm^{-1} in the fingerprint vibration spectrum region ($1500\text{--}600\text{ cm}^{-1}$).

- 4) After the high-viscosity modifier content reached 14%, the penetration of SBS-I and SBS-II high-viscosity asphalt decreased, and their growth trend of ductility and softening point also slowed. Considering the total cost, when the SBS-modified asphalt-high-viscosity modifier ratio is 86:14, the overall performance of high-viscosity asphalt is optimal.
- 5) According to the existing gradation design methods, two gradations are designed: PAC-1 and PAC-2. $VCA_{\text{mix}} < VCA_{\text{DRC}}$ and $SSC > 90\%$ were used to evaluate the two gradations. It was found that the VCA_{mix} of the four asphalt mixtures, PAC-1-I, PAC-1-II, PAC-2-I and PAC-2-II, were all smaller than VCA_{DRC} , and their SSCs were 105.08%, 104.74%, and 100.64% and 101.33%, respectively, indicating that the aggregates in the four mixtures form a skeleton-embedded structure.
- 6) According to the results of Cantabro and draindown tests, the optimal asphalt-aggregate ratios of PAC-1-I, PAC-1-II, PAC-2-I and PAC-2-II asphalt mixtures are 4.6%, 4.5%, 5.3%, and 5.3%, respectively.
- 7) The performance of the four asphalt mixtures designed was verified and found to meet the requirements. After considering all performances, the recommended optimal PUTO asphalt mixture type is PAC-1-II.

Declaration of Competing Interest

The authors declared that they have no conflicts of interest to this work.

Acknowledgements

This work was undertaken with funding from the National Natural Science Foundation of China (Program No. 51408125), sponsored by the Qing Lan Project and the “333” high level talent training project in Jiangsu. The opinions, findings, and conclusions expressed in this publication are those of the authors and not necessarily those of any organization.

References

- [1] W.S. Mogawer, A.J. Austerman, S. Underwood, Effect of binder modification on the performance of an ultra-thin overlay pavement preservation strategy, *Transp. Res. Rec.* 2550 (2016) 1–7.
- [2] J. Bellanger, Y. Brosseau, J.L. Gourdon, Thinner and thinner asphalt layers for maintenance of French roads, *Transp. Res. Rec.* 1334 (1992) 9–11.
- [3] H. Zhang, H. Li, Y. Zhang, D. Wang, J. Harvey, H. Wang, Performance enhancement of porous asphalt pavement using red mud as alternative filler, *Constr. Build. Mater.* 160 (2018) 707–713.
- [4] J. Chen, C. Lee, Y. Lin, Influence of engineering properties of porous asphalt concrete on long-term performance, *J. Mater. Civ. Eng.* 29 (4) (2017) 04016246.
- [5] L. Yao, X. Wang, Z. Cong, G. Cao, The application of TPS modified asphalts in granulated crumb rubber asphalt mixture, in: *International Conference on Mechanic Automation & Control Engineering*, IEEE, 2011, pp. 15–17. 12261234.
- [6] W. Zhang, J. Shi, Z. Jia, The UV anti-aging performance of TPS modified bitumen, *Pet. Sci. Technol.* 36 (15) (2018) 1164–1169.
- [7] Z. Chen, W. Yuan, D. Zheng, Application research of gradation theory, *J. Chongqing Jiaotong Univ.* 04 (2005) 44–48.
- [8] C.A. Weymouth, Effects of particle interference in mortars and concretes, *Rock Products* 36 (2) (1933) 26–30.
- [9] W.B. Fuller, S.E. Thompson, The laws of proportioning concrete, *Trans. Am. Soc. Civ. Eng.* 59 (1907) 67–143.
- [10] Y. Wang, Research on Gradation Optimization of Asphalt Mixture (A Doctoral Dissertation), Chang’an University, Xi’an, China, 2008.
- [11] M.L. Pattanaik, R. Choudhary, B. Kumar, Laboratory evaluation of mix design parameters of open-graded friction course mixes with electric arc furnace steel slag, *Adv. Civ. Eng. Mater.* 7 (1) (2018) 616–632.
- [12] Y. Peng, L. Sun, Evaluation method for uniformity of asphalt mixture based on fractal theory, *J. Harbin Inst. Technol.* 10 (2007) 1656–1659.
- [13] L. Xu, Research on Asphalt Mixture Design Method Based on New Skeleton Intrusion Principle (A Master Dissertation), Shandong Jianzhu University, Jinan, China, 2017.
- [14] X. Chou, A. Chegenizadeh, H. Nikraz, Evaluation of stone mastic asphalt mix by the Bailey method design, *Aust. Geomech. J.* 51 (2) (2016) 105–112.
- [15] L. Cheng, P. Hao, Design method of mother-asphalt-mixture with semi-flexible pavement based on the volume method, *J. Chang’an Univ. (Nat. Sci. Ed.)* 22 (1) (2002) 1–3.
- [16] Y. Tan, X. Zhang, Z. Guo, Design of mixing ratio of SMA mixture by volume method, *J. Harbin Univ. Construct.* 3 (1999) 105–110.
- [17] Z. Liu, S. Luo, X. Quan, X. Wei, X. Yang, Q. Li, Laboratory evaluation of performance of porous ultra-thin overlay, *Constr. Build. Mater.* 204 (2019) 28–40.
- [18] JTG F40-2004 Technical Specification for Construction of Highway Asphalt Pavement in China, General Administration of Quality Supervision, Inspection and Quarantine of the People’s Republic of China, Beijing, 2004.
- [19] JTG E20-2011 Standard Test Method of Bitumen and Bituminous Mixture for Highway Engineering in China, General Administration of Quality Supervision, Inspection and Quarantine of the People’s Republic of China, Beijing, 2011.
- [20] JTG E42-2005 Testing Procedures of Aggregate for Highway Engineering in China, General Administration of Quality Supervision, Inspection and Quarantine of the People’s Republic of China, Beijing, 2005.
- [21] M. Xing, Study on the properties of glue and mineral composition of asphalt mixture on drainage pavement. A Doctoral Dissertation of Chang’an University, Xi’an, China, 2010.
- [22] F. Zhang, C. Hu, Preparation and properties of high viscosity modified asphalt, *Polym. Compos.* 38 (5) (2015) 936–946.
- [23] Japan Road Association Drainage paving technology pointer, Maruzen Corporation, Tokyo, Japan, 1996.
- [24] Z. Pu, K. Chen, J. Wang, et al., Determination of SBS modifier content in SBS modified asphalt, 2016, Chinese Patent, 201610995830.1
- [25] C. Ai, Q. Shi, C. Xin, et al., Evaluation and optimisation of stone matrix asphalt (SMA-13) mixture design using weight-matrix method, *Road Mater. Pavement Des.* 17 (4) (2016) 958–967.
- [26] P. Hao, J. Xu, H. Zhou, Key techniques for gradation composition design by Beray method, *J. Chang’an Univ. (Nat. Sci. Ed.)* 6 (2004) 1–6.
- [27] J. Fang, Design and Application of Large Particle Size Drainage Asphalt Mixture (A Master Dissertation), Tongji University, Shanghai, China, 2006.
- [28] J. Qi, Research on Composition Design and Road Performance of Large Particle Size Permeable Asphalt Mixture, Wuhan University of Engineering, Wuhan, China, 2014.
- [29] B. Xu, J. Chen, C. Zhou, W. Wang, Study on Marshall Design parameters of porous asphalt mixture using limestone as coarse aggregate, *Constr. Build. Mater.* 124 (2016) 846–854.
- [30] ASTM standards D7175 Test Method for Determining the Rheological Properties of Asphalt Binder Using a Dynamic Shear Rheometer.